Author's Accepted Manuscript

www.elsevier.com/locate/talanta

Silica Nanoparticles Coated by Poly(acrylic acid) Brushes via Host-Guest Interactions for Detecting DNA Sequence of Hepatitis B Virus

Lu Ding, Chunlan Xiang, Gang Zhou

PII: S0039-9140(17)31266-3
DOI: https://doi.org/10.1016/j.talanta.2017.12.061
Reference: TAL18197

To appear in: *Talanta*

Received date: 25 October 2017
Revised date: 10 December 2017
Accepted date: 21 December 2017

Cite this article as: Lu Ding, Chunlan Xiang and Gang Zhou, Silica Nanoparticles Coated by Poly(acrylic acid) Brushes via Host-Guest Interactions for Detecting DNA Sequence of Hepatitis B Virus, *Talanta,* https://doi.org/10.1016/j.talanta.2017.12.061

Silica Nanoparticles Coated by Poly(acrylic acid) Brushes via Host-Guest Interactions for Detecting DNA Sequence of Hepatitis B Virus

*Lu Ding, Chunlan Xiang, and Gang Zhou**

Lab of Advanced Materials, State Key Laboratory of Molecular Engineering of Polymers, Collaborative Innovation Center of Chemistry for Energy Materials, Fudan University, Shanghai 200438, P. R. China.

***Corresponding author:** Prof. G. Zhou, Tel./Fax: +86-21-5163-0350.

E-mail: zhougang@fudan.edu.cn

Abstract

Poly(acrylic acid) (PAA) brushes coated onto silica nanoparticles have been widely utilized in bioassays due to their abilities of providing favorable microenvironments and ensuring good biological activities for biomolecules. However, traditional PAA brushes are synthesized by reversible addition–fragmentation chain transfer polymerization. Hence, it is generally difficult to control and characterize the molecular weight of the PAA brushes, which may depress the reproducibility and bring more uncertain results. Herein, atom transfer radical polymerization method is employed to synthesize β-cyclodextrin-cored PAA with uniform and controllable molecular weight. After loading on the surfaces of adamantane-functionalized silica nanoparticles via host-guest interactions, glucose oxidase and probe single strand DNA (ssDNA) are further immobilized on the as-prepared nanoparticles. Meanwhile, capture ssDNA is functionalized on amino modified magnetic beads. In the presence of ssDNA sequence of Hepatitis B Virus (HBV) containing completely matched sequence of both probe and capture ssDNA, a

bioconjugate is formed and can be separated by an external magnet. The isolated glucose oxidase can further catalyze glucose into gluconic acid and H_2O_2, and then reduce $HAuCl_4$ on Au seeds. By monitoring the absorption intensity change of the Au NPs at 530 nm, the proposed biosensor with novel signal amplification probes can be used to detect DNA sequence of HBV with high sensitivity and selectivity in both buffer and serum samples. This developed strategy has presented a new way to construct silica nanoparticles coated by PAA brushes for the fields of clinical diagnosis and other life sciences.

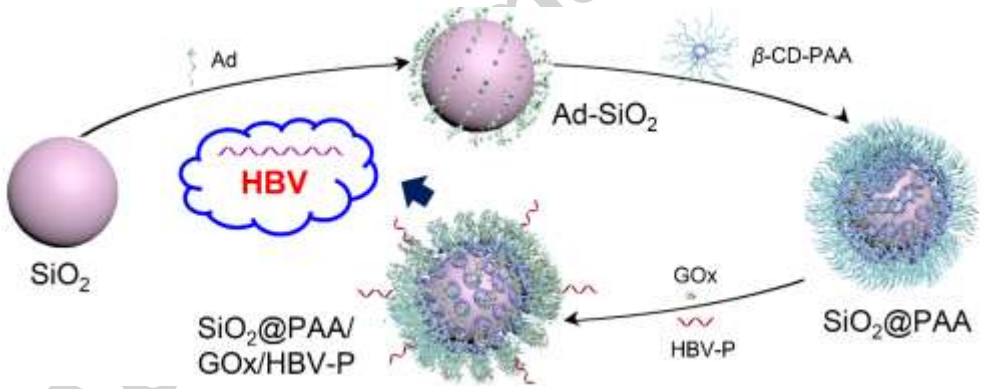

Graphical abstract

Key words: Poly(acrylic acid) Brush; Host-Guest; ATRP; Colorimetric Bioassay; Hepatitis B Virus.

1. Introduction

Infection with virus is one of the major health problems worldwide. Hepatitis B virus (HBV), which is highly infectious, can transmit through percutaneous route (i.e., puncture through the skin) or mucosal (i.e., direct contact with mucous membranes) exposure to infected blood or body fluids [1]. Meanwhile, HBV is one of the unambiguous human oncogenic viruses which may induce hepatocirrhosis, liver cancer, liver failure, and death [2-4]. Although the introduction of an effective vaccine against HBV has reduced its prevalence, the World Health Organization estimates that more than 2 billion people are HBV-infected and 350 million people are chronic carriers [5]. Therefore, the detection and quantification of HBV have become increasingly important in clinical medical practice. Hepatitis B surface antigen (HBsAg) and Hepatitis B e antigen (HBeAg) are mainly used to identify HBV [6-9]. However, in early phase of infection, both HBsAg and HBeAg are negative inside patient systems [10]. Consequently, the establishment of ultrasensitive methods is necessary for the early detection. The analysis of HBV nucleic acid sequence is more reliable than HBsAg and HBeAg for identification of HBV [11,12]. Recently, various biosensors have been developed to detect the DNA sequence of HBV, including electrochemistry assay [11,13], fluorescence assay [15,16], and enzyme-linked immunosorbent assay [17]. However, the sensitivity in some reported system is limited. Therefore, construction of highly sensitive biosensor for HBV detection is still a challenge work in this field.

To build highly sensitive bioassays, signal amplification strategies often require preprocessed probes. Different kinds of signal amplification methods have been used including entrapping method [18,19], physical adsorption [20,21], and covalently binding [22]. Polymers, containing large amounts of constitutional repeating units, are generally considered to be ideal signal amplification probe in bioassays. Among the various water-soluble polymers, poly(acrylic acid) (PAA) is always used to covalently bind bioenzymes due to its abundant content of carboxyl groups which can immobilize the biomolecules, control drug release, and so on [23-30]. Additionally,

PAA may provide favorable microenvironment and ensure good biological activity of the biomolecules [22,31]. In practical applications, PAA brushes are always loaded on biocompatible silica nanoparticles (NPs). However, such loaded PAA brushes are usually synthesized by reversible addition–fragmentation chain transfer (RAFT) polymerization on silica NPs [29], which makes it difficult to control and characterize the molecular weight of PAA. Moreover, a wide range of polydispersity index (PDI) leads to different contents of carboxyl groups, depressing the reproducibility of the bioassays.

Herein, PAA brushes with low PDI value are controllably polymerized via atom transfer radical polymerization method [32,33]. After loading on the surfaces of adamantane-functionalized silica NPs via host-guest interactions, glucose oxidase (GOx) and probe single strand DNA (ssDNA) of HBV are successively functionalized onto the as-prepared nanoparticles. Synchronously, capture ssDNA of HBV was immobilized on amino modified magnetic beads. Only in the presence of HBV ssDNA containing completely matched sequences of both probe and capture ssDNA of HBV, double strand DNA was formed, which connected the magnetic beads and the silica NPs. Therefore, when the formed bioconjugate was separated by an external magnet, the isolated GOx could catalyze glucose into gluconic acid and H_2O_2 [34,35], and then reduce $HAuCl_4$ on Au seeds [36,37]. Consequently, by monitoring the absorption intensity change of the Au NPs at 530 nm [38], the amount of the detected HBV ssDNA could be quantified.

2. Experimental section

2.1 Materials and reagents

Glucose oxidase, *β*-cyclodextrin hydrate (*β*-CD), 2-bromoisobutyryl bromide, 1-(3-dimethylaminopropyl)-3-ethylcarbodiimide hydrochloride (EDC), and 1-hydroxy-2,5-pyrrolidinedione (NHS) were purchased from J&K Scientific Ltd. Glutaric dialdehyde was obtained from Aladdin Industrial Inc. Chloroauric acid was purchased from Shanghai Sinopharm chemical reagent company. Adamantanamine

was obtained from Acros Organics. Tetraethyl orthosilicate and 3-glycidoxypropyltrimethoxysilane were purchased from Energy Chemical Inc. Aminated magnetic beads (MBs) were obtained from XFNANO Ltd. All chemicals in this study were obtained from the manufactures without purification unless specifically noted. Cross-linking buffer was 2-(*N*-morpholino)ethanesulfonic acid buffer (MES buffer, 10 mM, pH = 5.0) containing 0.05 wt% Tween-20, which was used to immobilized GOx. Hybridization buffer was Tris/HCl buffer (TBS buffer, 10 mM, pH = 8.0) containing 150 mM NaCl and 5mM $MgCl_2$. Test buffer was citrate-Na_2HPO_4 buffer (10 mM, pH = 5.0). The pH measurement was carried out on a Mettler-Toledo Delta FiveGo pH meter. Deionized water (MillQ, 18.2 MΩ) was used throughout the study. The serum samples were kindly provided by Shanghai General Hospital and stored at 4 °C. DNA oligonucleotide and bovine serum albumin (BSA) used in this work were synthesized and purified by Sangon Biotech Co., Ltd., and the sequence is shown as follows:

Target ssDNA sequence related to HBV:

HBV-T: 5′-ATA CCA CAT CAT CCA TAT AAC TGA AAG CCA-3′

Capture ssDNA sequence:

HBV-C: 5′-TGG ATG ATG TGG TAT-C6-NH_2-3′

Probe ssDNA sequence:

HBV-P: 5′-NH_2-C6-TGG CTT TCA GTT ATA-3′

Mismatched ssDNA sequences for HBV:

HBV-MT1: 5′-ATA CCA CAT CAT CCA **A**AT AAC TGA AAG CCA-3′

HBV-MT3: 5′-ATA C**G**A CAT CA**A** CCA TAT AAC **A**GA AAG CCA-3′

Random ssDNA sequences:

R1: 5′- TCC GAA TAG GGC CCC -3′

R2: 5′- GGG GCC CTA TTC GGA GTG AGC AGG GGA GAG -3′

2.2 Characterizations

^{1}H NMR (400 MHz) spectra were measured on a Varian Mercury Plus-400 spectrometer. Gel permeation chromatography was operated using an Agilent 1100

system equipped with both G1362A refractive-index and G1314A UV detectors (eluent: THF; calibration: polystyrene standards). Fourier transform infrared (FTIR) spectra were recorded from IRAffinity spectrometer (Shimadzu, Japan). The scan number was 32 throughout the study. Transmission electron microscopy (TEM) images were obtained from JEM-2100F electron microscope (JEOL, Japan, 200 kV). Ultraviolet−visible (UV-vis) absorption spectra were obtained from UV-2550PC spectrometer (Shimadzu, Japan). The UV-vis measurements were performed in a 1 mm quartz cuvette with the slit of 1.0 under fast scan speed. The solution volume for each measurement was 200 µL. Dynamic light scattering (DLS) and Zeta potentials were measured by Zetasizer Nano ZS (Malvern, UK) particle size analyzer. DLS and Zeta potentials were measured at 25 °C with 15 scans.

2.3 Synthesis

2.3.1 Synthesis of SiO_2 nanoparticles

SiO_2 nanoparticles were prepared by a slightly modified Stöber process [39]. In a typical synthesis of 120 nm SiO_2 nanoparticles, 4.5 mL of tetraethyl orthosilicate was rapidly added into a mixture of 62 mL of anhydrous ethanol, 25 mL of deionized water and 9 mL of NH_3•H_2O (28%). The mixture was vigorously stirred for 2 h. Finally, the monodisperse SiO_2 NPs were separated by centrifugation and washed with ethanol for several times to remove impurities. Dry SiO_2 NPs were obtained by drying the residue at 45 °C in vacuum.

2.3.2 Synthesis of adamantane-based silane coupling agent (Ad-Si)

The Ad-Si was prepared by previous literature [40]. Adamantanamine (6.61 mM) was dissolved in 30 mL dry methanol. The mixture was stirred until all solids disappeared, then 6.35 mM 3-glycidoxypropyltrimethoxysilane was added at room temperature. The reaction mixture was refluxed overnight at the nitrogen atmosphere. The product was used for the next step without further purification.

2.3.3 Synthesis of Ad-Si modified SiO_2 nanoparticles (Ad-SiO_2 NPs)

SiO_2 NPs (0.05 g), Ad-Si (0.5 mL), and dry toluene (25 mL) were placed in a dried flask. The resultant mixture was allowed to be warmed up to 110 °C and

vigorously stirred for 24 h under N_2 atmosphere. The modified Ad-SiO_2 NPs were separated by centrifugation and washed with anhydrous toluene and ethanol for several times to remove impurities. The product was dried under vacuum overnight.

2.3.4 Synthesis of heptakis[2,3,6-tri-o-(2-bromo-2-methyl-propionyl]-*β*-cyclodextrin (Br-*β*-CD)

The Br-*β*-CD was prepared according to previous published literatures [33,41]. *β*-CD (3 mM) was dissolved in anhydrous 1-methyl-2-pyrrolidione (NMP) and was cooled to 0 °C. Then 126 mM 2-bromoisobutyryl bromide was added dropwise to the mixture with magnetic stirring. The reaction temperature was maintained at 0 °C for 2 h. Subsequently, it was allowed to be warmed up to room temperature and stirred for another 22 h under the nitrogen atmosphere. The brown reaction solution was concentrated under vacuum overnight. The reaction product was diluted with dichloromethane, and then washed sequentially with saturated $NaHCO_3$ aqueous solution and deionized water for several times to remove excess 2-bromoisobutyryl bromide. The organic layer obtained was concentrated in a vacuum oven, and then crystallized in cold *n*-hexane to produce a white precipitate. ^{1}H NMR (400 MHz, $CDCl_3$, δ ppm): 1.2-2.4 (m), 3.5-4.9 (m), 5.25 (m).

2.3.5 Synthesis of *β*-cyclodextrin-PtBA (*β*-CD-PtBA)

Polymerization of *tert*-butylacrylate (tBA) was performed using Br-*β*-CD as a macroinitiator possessing ATRP initiation sites [42]. All polymerizations were performed in an ampoule. The reaction mixtures with CuBr (0.1414g), PMDETA (0.0341 g), Br-*β*-CD (0.025 g), tBA (8.58 mL), and 8.6 mL methylethylketone was vacuumed by three freeze-thaw-cycles in liquid N_2, as the typical polymerization procedure. The resultant mixture was stirred under N_2 atmosphere at 60 °C. The mixture was then diluted with acetone and passed through a column of neutral alumina to remove the catalyst. The product was precipitated in the mixed solvents of methanol/water (v/v = 1/1), filtered, and dried at 40 °C in vacuum [32]. ^{1}H NMR (400 MHz, $CDCl_3$, δ ppm):1.39 (s), 1.48-2.17 (m). $M_n = 4.95\times10^5$, PDI = 1.16.

2.3.6 Synthesis of *β*-cyclodextrin-PAA (*β*-CD-PAA)

In a typical process, star-like *β*-CD-PtBA (0.3 g) was dissolved in 30 mL CH_2Cl_2,

and then 10 mL trifluoroacetic acid was added. The reaction mixture was stirred at room temperature for 24 h. After the hydrolysis, the product *β*-CD-PAA was dissolved in methanol and then precipitated in CH_2Cl_2, filtered, and dried at 40 °C in vacuum. ^{1}H NMR (400 MHz, D_2O, *δ* ppm): 1.47-1.78 (m), 2.26 (s)

2.3.7 Synthesis of SiO_2@PAA NPs

Amount of the synthesized *β*-CD-PAA and Ad-SiO_2 NPs were dispersed in deionized water, respectively. Then the excess *β*-CD-PAA solution was added into the Ad-SiO_2 NPs and reacted for 1 h. The resulting mixture was centrifuged and washed with ethanol and deionized water for several times. After removing the excessive star-like *β*-CD-PAA, the obtained SiO_2@PAA NPs were dried at 40 °C in vacuum.

2.3.8 Synthesis of Au seeds

1 mL of 0.1 mM $HAuCl_4$ was added to 1 mL of 0.5mM sodium citrate at room temperature. After 1 min of stirring, 60 μL of fresh 0.1 M $NaBH_4$ was added. The colloidal solution was stirred for an additional 30 min and stored at 4 °C [43].

2.4 Fabrication of the biosensor probe (SiO_2@PAA/GOx/HBV-P NPs)

The SiO_2@PAA/GOx NPs were synthesized by covalently immobilizing GOx in SiO_2@PAA NPs using the "chemical conjugation after electrostatic entrapment" (CCEE) process [44]. SiO_2@PAA NPs (30 mg) were dispersed into 5 mL of MES buffer and mixed with GOx for 20 min at room temperature. After removing the excessive GOx by centrifugation, 1 mL of EDC (0.5 mM) was added to the mixture, and shaken for 2 h at room temperature. The above bioconjugate was washed with MES buffer and dispersed with a concentration of 30 mg/mL for further use.

The amino modified probe (HBV-P) was conjugated to the edge of the brushes via NHS/EDC process. In accordance with conventional experiment, EDC and NHS (100 mM) were added into 1 mL of the as-prepared SiO_2@PAA/GOx NPs. After centrifugation three times with MES buffer, 50 μL of HBV-P (5 μg/mL) was added and stirred for 2 h at 37 °C. The above bioconjugate was washed and blocked with 1 wt% BSA then stored at 4 °C with a final concentration of 3 mg/mL.

2.5 Fabrication of the capture probe (MB/HBV-C)

The amino modified magnetic beads (MBs) were used to fabricate capture oligonucleotide. In a typical process, 1 mL of MBs solution (1 mg/mL) was mixed with 1 mL of HBV-C (20 μg/mL), then 2.5% glutaric dialdehyde solution was added into the above mixture and shaken for 1 h at room temperature. The resultant MB/HBV-C was separated using magnet and re-dispersed in TBS buffer (1 mg/mL) after being washed. The obtained capture probe was incubated in 1 wt% BSA for 2 h at room temperature and stored in TBS buffer (0.1 M) at 4 °C for further use.

2.6 Preparation of the biosensor

The capture DNA (HBV-C) was firstly immobilized on amino modified magnetic beads (MBs), and then incubated with BSA to block nonspecific binding site. Then various amounts of HBV-T were added into the capture probe MB/HBV-C and incubated at 37 °C in TBS buffer for 30 min. After being washed and separated by magnet with TBS buffer, the synthesized SiO_2@PAA/GOx/HBV-P NPs probe were added and incubated for 30 min under the same condition. In the presence of target ssDNA (HBV-T) containing completely matched sequences of both probe ssDNA (HBV-P) and capture ssDNA (HBV-C), double strand DNA (dsDNA) was formed. The bioconjugate was washed with citrate-Na_2HPO_4 buffer and separated by magnet. Future 5 mM glucose mixed with 5 nm Au seeds and HAuCl4 were added in the bioconjugate and incubated at 37 °C in Citrate-Na_2HPO_4 buffer for 10 min. Based on the change of the increased extinction coefficient at 530 nm of Au NPs, the resulted solution was measurement in UV-vis absorption spectrum.

3. Results and discussion

3.1 Synthesis and Characterization of the Probe Based on SiO_2@PAA NPs

The synthetic strategy of the probe is illustrated in **Scheme 1**. Initially, SiO_2 nanospheres were prepared from tetraethyl orthosilicate via a slightly modified Stöber process [39]. Then adamantane-based silane coupling agent Ad-Si (**Scheme 2**) [40,45]

was covalently linked onto the surface of the as-prepared SiO_2 NPs. Synchronously, according to Lin's method [32], *β*-CD with 21 hydroxyl groups was esterified by end-capping the hydroxyl groups with 2-bromoisobutyryl bromide, which produces the star-like macroinitiator (**Scheme 3**). Subsequently, *β*-CD-PtBA was prepared by

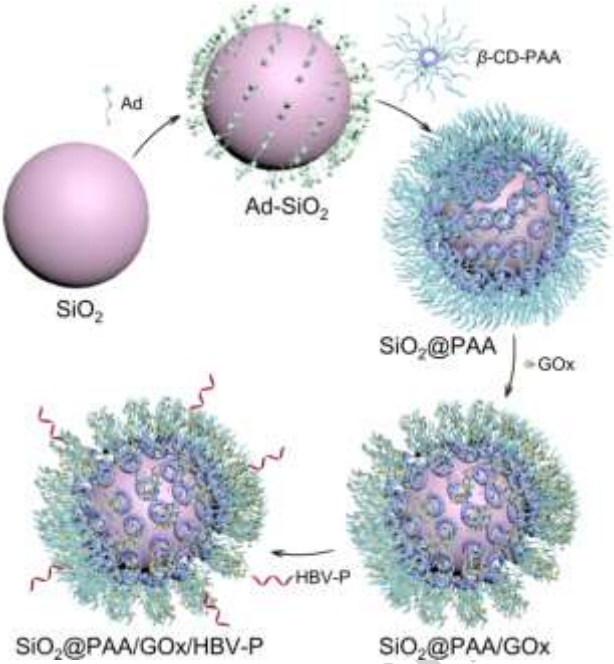

Scheme 1. Schematic illustration of the preparation of the probe based on SiO_2@PAA/GOx/HBV-P NPs.

ATRP method with the assistance of the initiator [32,33]. The numeric molecular weight was determined to be 4.95×10^5 Da and PDI to be 1.16 by gel permeation chromatography (GPC) measurement (**Figure S1**). Then, *β*-CD-PAA was produced by hydrolyzing *β*-CD-PtBA in the presence of trifluoroacetic acid (**Scheme 3**). The successful hydrolyzation of *β*-CD-PtBA to *β*-CD-PAA was validated by the complete disappearance of the singlet signal at δ = 1.29 ppm [32], corresponding to the protons in the *tert*-butyl groups. The prepared *β*-CD-PAA consists of a *β*-CD core and PAA brushes surrounding it. Therefore, it can be well dispersed in aqueous solution. It is well known that *β*-CD, a macrocyclic cavitand consisting of seven glucopyranose units, has a hydrophobic cavity that can serve as a perfect receptor for an adamantane group [46-48]. Consequently, the SiO_2@PAA NPs were provided via host-guest interactions between adamantane-functionalized silica nanospheres and *β*-CD-cored

PAA micelles. The as-prepared SiO_2@PAA NPs were abundant in carboxyl groups in the PAA shell, which made it possible to immobilize GOx for further bioassays. After loading GOx via CCEE process [49], the SiO_2@PAA/GOx NPs were functionalized with probe ssDNA (HBV-P) via the NHS/EDC process and thus the probe based on SiO_2@PAA/GOx/HBV-P NPs is obtained (**Scheme 1**).

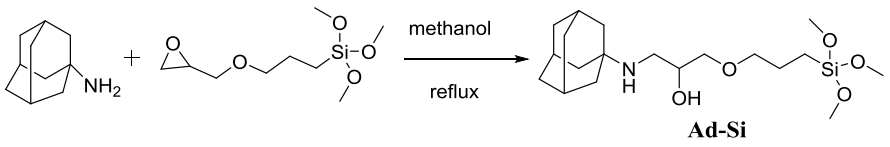

Scheme 2. Synthetic route of silane coupling agent Ad-Si.

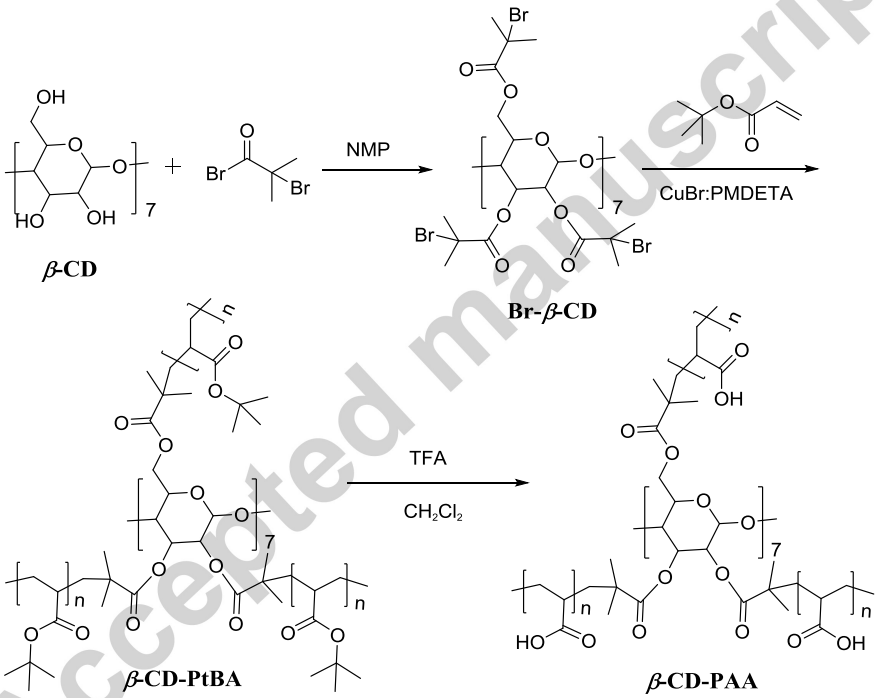

Scheme 3. Synthetic route of *β*-CD-PAA.

To prove the successful loading of PAA micelles on the surface of SiO_2 nanospheres, FTIR spectra of SiO_2, Ad-SiO_2, *β*-CD-PAA, and SiO_2@PAA NPs were recorded. As shown in **Figure 1**, the as-prepared SiO_2 NPs displays a sharp peak at 1102 cm^{-1} and a rather broad peak at 3425 cm^{-1}, attributed to the stretching vibration of Si-O and O-H bond, respectively [40]. When the adamantane-functionalized silane

coupling agent is covalently linked onto the surface of SiO_2 nanospheres, the Ad-SiO_2 NPs exhibit a rather broad peak at 3425 cm^{-1}, which indicates that the O-H groups located on the SiO_2 NPs have reacted with the silane coupling agent. For β-CD-PAA micelles, a weak band peaked at 1727 cm^{-1} is assigned to the stretching vibration of C=O bond [49,50]. Upon the formation of SiO_2@PAA NPs via host-guest interactions, both characteristic vibration bands of β-CD-PAA and Ad-SiO_2 NPs can be found in the FTIR spectrum, which suggests the successful combination of β-CD-PAA and Ad-SiO_2 NPs.

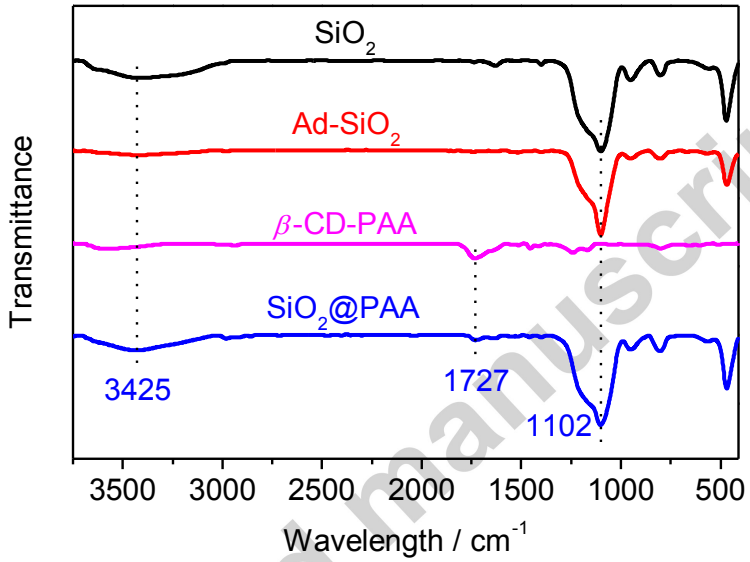

Figure 1. FTIR spectra of SiO_2, Ad-SiO_2, β-CD-PAA, and SiO_2@PAA NPs.

The morphology of the synthesized SiO_2 and SiO_2@PAA NPs were characterized by TEM. As shown in **Figure 2a**, the monodispersed SiO_2 NPs exhibited a good spherical shape and uniform size with an average diameter of 120 nm. When β-CD-PAA was attached onto the surfaces of adamantane-functionalized SiO_2 NPs, a core-shell structure can be observed for SiO_2@PAA NPs, as shown in **Figure 2b**. The PAA shell capped on the SiO_2 core exhibits an average thickness of 30 nm. The size distributions of these NPs were further analyzed by DLS measurements. As revealed in **Figure 2c**, uniform morphologies can be found for SiO_2, β-CD-PAA, and SiO_2@PAA NPs. The as-prepared SiO_2 NPs demonstrate a particle size of 120 ± 30 nm in MES buffer, while the size distribution of β-CD-PAA is 58 ± 20 nm. As

expected, when the SiO_2 NPs are packed by β-CD-PAA, the SiO_2@PAA NPs display a particle size of 190 ± 30 nm. This indicates the successful coverage of PAA layer on the surface of SiO_2 NPs. It should be noted that the particle sizes were slightly different from those measured by TEM and probably caused by the shrinkage and accumulation of micelle during the drying process [51]. To further prove the combination between Ad-SiO_2 and β-CD-PAA, the zeta potentials of these NPs were measured in anhydrous ethanol. The SiO_2 NPs showed in a zeta potential of -9 mV due to the surrounded hydroxyl group on the particle surfaces [52]. Upon the attachment of adamantine units onto the surfaces of SiO_2 NPs, the zeta potential of Ad-SiO_2 NPs evidently changed to 36 mV owing to the introduction of amino groups. Under the same condition, the β-CD-PAA micelles exhibited a zeta potential of -14 mV due to the large amount of carboxylic acid groups. When the β-CD-PAA micelles interacted with Ad-SiO_2 NPs via host-guest interactions, a negatively shifted zeta potential of -48 mV was obtained, which proved the encapsulation of the hydrophobic adamantine units into the cavity of β-CD.

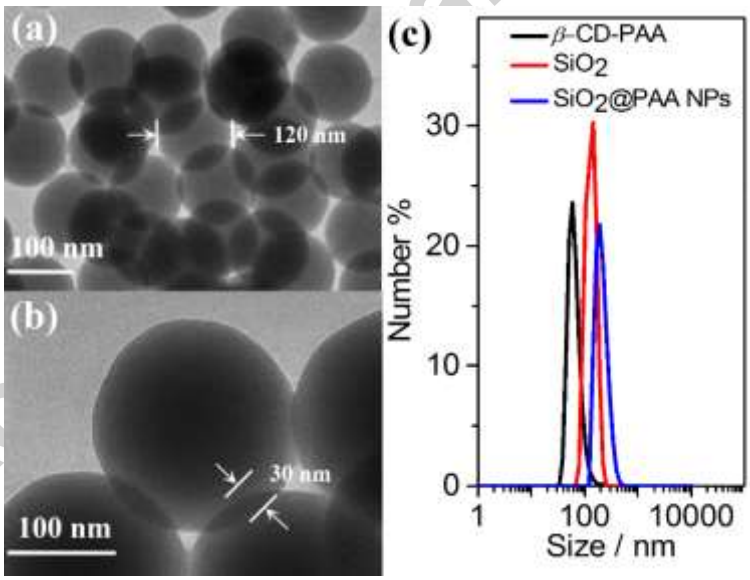

Figure 2. TEM images of (a) SiO_2 and (b) SiO_2@PAA NPs, and (c) size distribution of β-CD-PAA, SiO_2, and SiO_2@PAA NPs.

The further immobilization of enzymes into SiO_2@PAA NPs was verified by UV-vis absorption spectra. As shown in **Figure S2**, GOx display two characteristic

absorption bands at 367 and 454 nm, respectively, which can be clearly observed as absorption shoulders in the absorption spectrum of SiO_2@PAA/GOx NPs as compared with that for SiO_2@PAA NPs. This suggests the successful loading of GOx into SiO_2@PAA NPs.

3.2 Sensing Mechanism

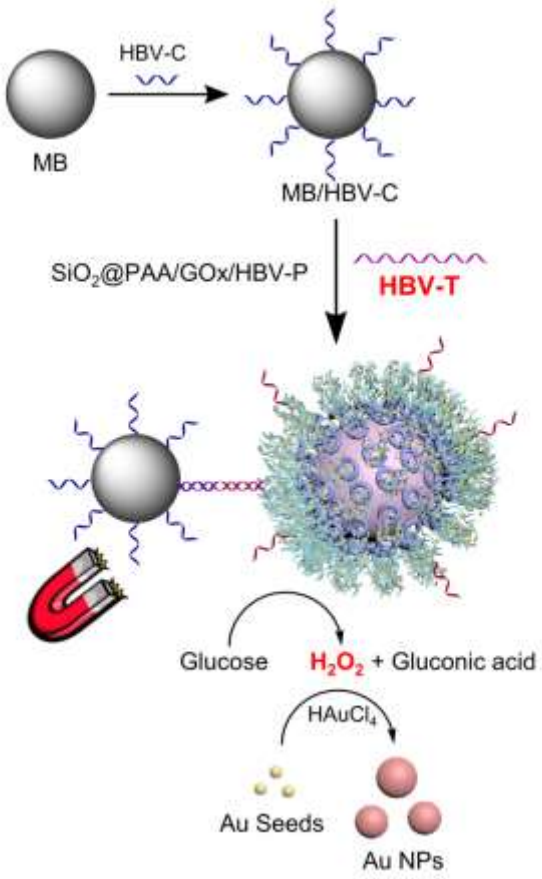

Scheme 4. Schematic illustration of the sensing mechanism for the nucleic acid sequence of HBV (HBV-T).

The sensing strategy of the biosensor for HBV is illustrated in **Scheme 4**. The capture DNA (HBV-C) was firstly immobilized on amino modified magnetic beads (MBs), and then incubated with BSA to block nonspecific binding site. In the presence of target ssDNA (HBV-T) containing completely matched sequences of both probe ssDNA (HBV-P) and capture ssDNA (HBV-C), double strand DNA (dsDNA) was formed, which connected the MBs and the SiO_2@PAA/GOx NPs. Therefore,

when the formed bioconjugate was separated by an external magnet, the amount of the detected target ssDNA was proportional to the separated GOx, which could be determined by additionally incorporated Au seeds. It is well known that glucose can be converted into gluconic acid and H_2O_2 with the assistance of GOx and oxygen. The produced H_2O_2 can reduce $HAuCl_4$ to Au^0 which may deposit around the Au seed and cause the growth of Au NPs [36,37]. Herein, uniform and monodispersed Au NPs with diameter of around 5 nm (TEM image shown in **Figure S3a**) were synthesized and served as Au seeds in this bioassay. When the separated GOx generated H_2O_2, the added $HAuCl_4$ was reduced and large size Au NPs were obtained (TEM image shown in **Figure S3b**). Meanwhile, the colorless solution changed to red because of the increased extinction coefficient at 530 nm of Au NPs (**Figure S3d**) [38], which could be used to quantify the target analytes. On the contrary, when mismatched DNA sequence was analyzed, no related bioconjugate could be formed between the MBs and the probe. Therefore, at the absent of GOx, the $HAuCl_4$ could not be reduced, which means that no obvious change of the UV-vis absorption spectrum can be detected for the Au NPs.

3.3 Optimization of Sensing Conditions

To achieve the highest sensitivity for the biocatalytic reaction, several sensing parameters were optimized. As a starting point, the pH value of the buffer and the incubation time were firstly optimized. **Figure 3a** displays the absorption intensity change of the Au NPs at 530 nm in citrate-Na_2HPO_4 buffer with different pH values. When the separated bioconjugate was mixed with glucose (5 mM), Au seeds (~5 nm size, 10 nM), and $HAuCl_4$ (0.2 mM), and incubated at 37 °C in citrate-Na_2HPO_4 buffer, the absorption intensity of the Au NPs at 530 nm gradually increases with the elevating pH value from 3 to 5 and then decreases at a lower speed with the pH value continuously elevating to 7. Moreover, the sensitivity of the bioassay was influenced by the incubation time. As shown in **Figure 3b**, the absorption intensity of the Au NPs at 530 nm reaches a plateau after incubation for 10 min. Therefore, the sensing properties of the bioassays were investigated in citrate-Na_2HPO_4 buffer with pH value

of 5 and incubation time of 10 min. Furthermore, the concentrations of Au seed and $HAuCl_4$ were optimized to realize the best performance of the bioassay. As shown in **Figure 4**, when the concentration of Au seed and $HAuCl_4$ is 9 nM and 0.2 mM, respectively, the most notable absorption intensity change is achieved in the sensing system. Consequently, the bioassays were conducted with the concentration of Au seed and $HAuCl_4$ equal to 9 nM and 0.2 mM, respectively, in citrate-Na_2HPO_4 buffer (pH = 5).

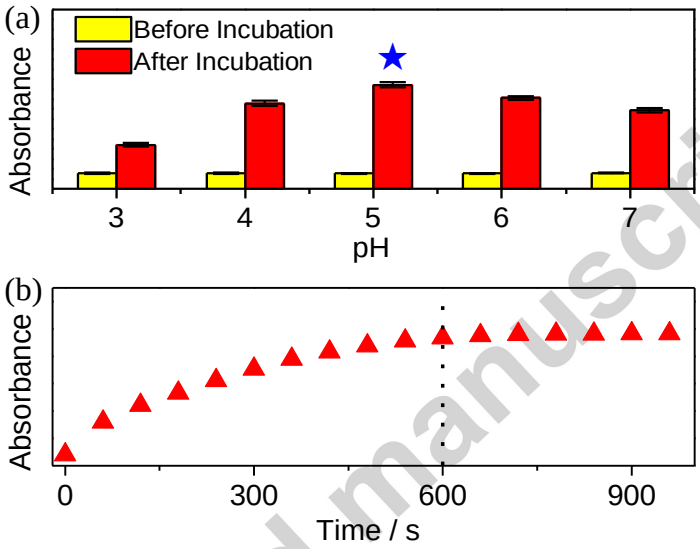

Figure 3. Absorption intensity of the Au NPs at 530 nm in citrate-Na_2HPO_4 buffer with different (a) pH values and (b) incubated time. The optimal conditions is pH = 5 and incubated time = 10 min. Error bars are estimated from six replicate measurements.

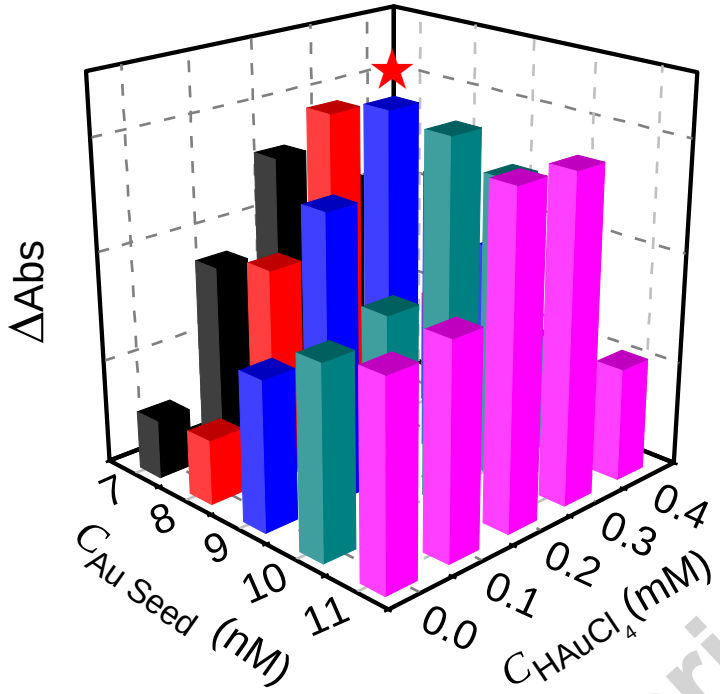

Figure 4. Absorption intensity changes of the Au NPs at 530 nm in the bioassays with different concentrations of Au seed and $HAuCl_4$. The optimal conditions is $C_{Au\ seed}$ = 9 nM and C_{HAuCl4} = 0.2 mM

3.4 Analytical Performance of the Biosensor for HBV-T

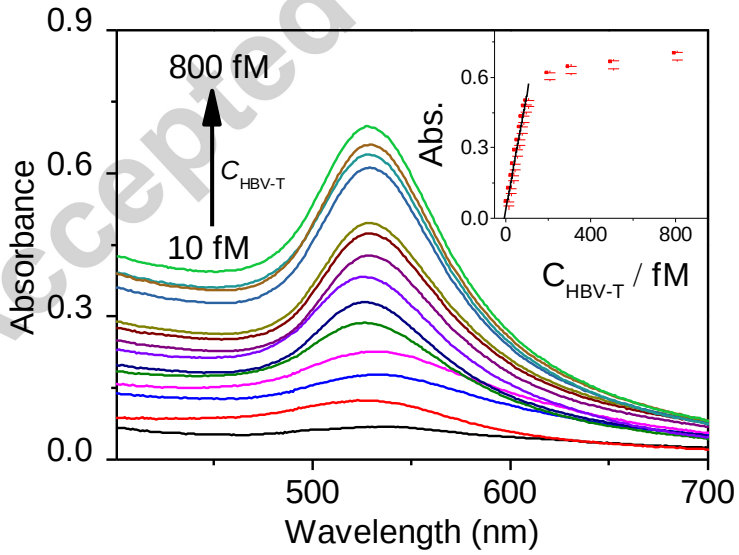

Figure 5. UV-vis absorption spectra of the Au NPs with different concentrations of HBV-T in citrate-Na_2HPO_4 buffer. Inset illustrates the absorbance at 530 nm versus HBV-T concentration. Error bars are estimated from six replicate measurements.

Under the optimized conditions, high sensitivity of the as-prepared probe towards HBV-T detection was achieved. The results were conducted by sextuplicate tests for each measurement, and the standard deviations were shown as error bars. As shown in **Figure 5**, the UV-vis signal at 530 nm is enhanced as the concentration of HBV-T increases. A good linear relationship between the absorption intensity and the HBV-T concentration can be found in the range of 10 – 100 fM (HBV-T liner concertration). The detection limit at a signal-to-noise ratio (S/N) of 3/1 is determined to be 3 fM. The linear regression equation is Y = 0.00495X + 0.0264 with a correlation coefficient (R^2) of 0.995 (black line in **Figure 6**). The high sensitivity can be attributed to signal amplification effect. The synthesized silica nanoparticles are covered by PAA brushes with high molecular weight. The rich content of carboxyl groups is utilized to immobilize GOx. When one ssDNA of HBV is detected, a bioconjugate containing a silica nanoparticle covered by numerous GOx molecules is formed. More GOx can produce more H_2O_2 and reduce more $HAuCl_4$ on Au seeds [36,37]. By monitoring the absorption change of the Au nanoparticles, the DNA sequence of HBV can be thus detected with high sensitivity.

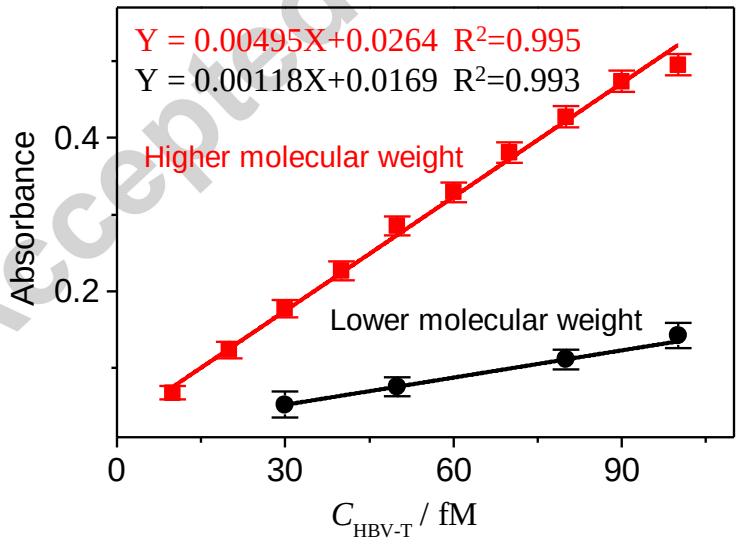

Figure 6. Calibration curves of the absorbance (λ = 530 nm) at varied concentrations of HBV-T using the probe based on PAA with different molecular weights. The black and red lines represent two PAA samples hydrolyzed from the precursors PtBA with

molecular weight of 4.95×10^5 and 9.76×10^4, respectively. Error bars are estimated from six replicate measurements.

To take advantage the preparation of PAA brush via ATRP method, a controlled *β*-CD-PAA with lower molecular weight was synthesized as reference and utilized in this bioassay. Comparatively lower response was obtained, as indicated in **Figure 6** (red line), the lower molecular weight probe exhibited linearity for HBV-T concentration. The linear regression equation is Y = 0.00118X + 0.0169 with a correlation coefficient (R^2) of 0.993. By comparing the slope values of the linear curves, the higher molecular weight probe exhibited an approximate 4.1-fold higher response rate than that of the lower molecular weight probe, which leads to the conclusion that the signal amplification increases with polymer molecular weight. For the PAA-based system with higher molecular weight, more GOx are immobilized in the SiO_2@PAA NPs due to the enhanced amount of carboxylic groups. In the presence of the biomaterial containing completely matched DNA sequences of both HBV-P and HBV-C, more $HAuCl_4$ can be reduced and higher absorption intensity of the Au NPs can be observed. Consequently, the probe based on PAA with higher molecular weight exhibit amplified sensitivity in comparison to that with lower molecular weight.

A high selectivity for the target analyte is an important requirement for a biosensor concerning their further practical applications. To investigate the specificity of the proposed biosensor, a single–mismatch sequence (HBV–MT1), a three–mismatch sequence (HBV–MT3), and random ssDNA sequences (R1 and R2) of HBV-T ssDNA were investigated by comparing the absorption intensity of the Au NPs at 530 nm under the same conditions. In these experiments, the solution was incubated with HBV-T (50 fM) or the above control sequences (500 fM), and then the signal changes of the UV-vis absorption spectra for the system were monitored. As shown in **Figure 7**, the intensity is slightly affected by the above control substances.

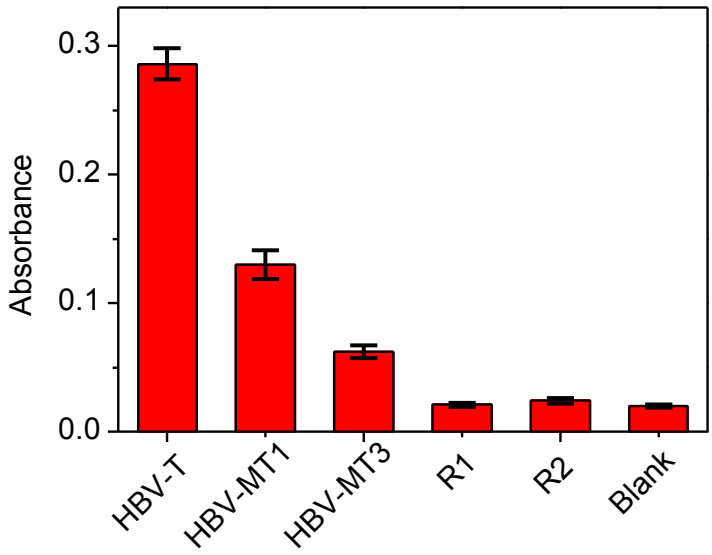

Figure 7. Selectivity of the biosensor for HBV-T detection. The concentration of other interfering substance was 500 fM and the HBV-T was 50 fM. Error bars are estimated from six replicate measurements.

In order to test the repeatability of the proposed biosensor, two different concentrations of HBV-T, 20 and 90 fM, were tested by twenty independently prepared biosensors. As shown in **Figure S4**, the value of relative standard deviation (RSD) was calculated and determined to be 1.9% and 3.9% respectively, which illustrates the acceptable precision and reproducibility for the biosensor. Furthermore, the stability of the biosensor is also a key factor in the practical application. A stability check was performed on the SiO_2@PAA/GOx/HBV-P NPs which were stored in buffer at 4 °C for 30 days. The experimental results showed that around 91% of the initial sensitivity was remained after 30 days. The excellent stability of the nanoparticles was due to the PAA brushes incorporated enzymes, which could prevent enzymes denaturation and leakage.

3.5 Application Analysis in Serum Samples

In order to evaluate the feasibility of the sensing system in complex biological samples, the assay of HBV-T was conducted in serum samples, a real complex media containing a variety of proteins and other contaminants. Different samples were

prepared by adding HBV-T with a certain concentration into the diluted human serum samples (1%). As indicated in **Table S1**, 20, 50, and 100 fM of HBV-T were added into the serum samples, respectively. The recovery of HBV-T was ranged from 93.9 ± 0.95% to 97.8 ± 1.92%, and the relative standard deviation (RSD) from 1.93% to 3.9%. These results indicated that the proposed biosensor possesses the promising applications in real biological matrices for detecting HBV.

4. Conclusion

In summary, *β*-CD-cored star-like PAA with uniform molecular weight was straightforward synthesized by ATRP method and successfully loaded on the adamantane-functionalized SiO_2 surface via host-guest interactions. After immobilizing GOx and further functionalizing HBV-P on the prepared SiO_2@PAA NPs, the resultant probe SiO_2@PAA/GOx/HBV-P NPs could be utilized as highly sensitive and selective biosensor for detecting DNA sequence of HBV (HBV-T). Only in the presence of target ssDNA (HBV-T) containing completely matched ssDNA sequences of both HBV-P and HBV-C, a bioconjugate was formed and separated by an external magnet. The isolated GOx could catalyze glucose into gluconic acid and H_2O_2, and indirectly reduce $HAuCl_4$ on Au seeds. By comparing the absorption intensity of the Au NPs at 530 nm, the amount of target ssDNA could be thus quantified. The detection limit at an S/N of 3/1 is determined to be 3 fM. Moreover, under the same condition, no obvious or slight absorption change could be observed for the ssDNA with random or mismatched sequences. Since the developed biosensor exhibited satisfactory reproducibility and stability, the proposed strategy could be further applied to detecting HBV-T in serum, which was of great importance in diagnosis and therapy of HBV infection. Overall, this work will facilitate the preparation of silica nanoparticles coated by PAA brushes with uniform and controllable molecular weight for the fields of clinical diagnosis and other life sciences.

Acknowledgements

This work was financially supported by the National Natural Science Foundation of China (51722301 and 21674023).

Supporting Information

Characterizations of the biosensor based on SiO_2@PAA NPs and the related sensing properties. This material is available free of charge via the Internet at http://www.sciencedirect.com

References

[1] E. E. Mast, C. M. Weinbaum, A. E Fiore, M. J. Alter, B. P. Bell, L. Finelli, L. E. Rodewald, J. M. Douglas, R. S. Janssen, J. W Ward, A comprehensive immunization strategy to eliminate transmission of Hepatitis B Virus infection in the United States - recommendations of the advisory committee on immunization Practices (ACIP) part II: Immunization of adults. Morb. Mortal. Wkly. Rep.55 (2006) 1-33.

[2] X. Li, Y. Huang, C. Song, M. Zhao, Y. Li, Several concerns about the primer design in the universal molecular beacon real-time PCR assay and its application in HBV DNA detection, Anal. Bioanal. Chem. 388 (2007) 979-985.

[3] S. Yates, M. Penning, J. Goudsmit, I. Frantzen, B. Van de Weijer, D. Van Strijp, B. Van Gemen, Quantitative detection of Hepatitis B Virus DNA by real-time nucleic acid sequence-based amplification with molecular beacon detection, J. Clin. Microbiol. 39 (2001) 3656-3665.

[4] L. Liu, X.Wang, Q. Ma, Z. Lin, S. Chen, Y. Li, L. Lu, H. Qu, X. Su, Multiplex electrochemiluminescence DNA sensor for determination of Hepatitis B Virus and Hepatitis C Virus based on ulticolor quantum dots and Au nanoparticles, Anal. Chim. Acta 916 (2016) 92-101.

[5] C. Stasi, C. Silvestri, F. Voller, F. Cipriani, The epidemiological changes of HCV and HBV infections in the era of new antiviral therapies and the anti-HBV vaccine, J. Infect. Public Heal. 9 (2016) 389-395.

[6] J. Shen, Y. Zhou, F. Fu, H. Xu, J. Lv, Y. Xiong, A. Wang, Immunochromatographic assay for quantitative and sensitive detection of hepatitis B virus surface antigen using highly luminescent quantum dot-beads, Talanta 142 (2015) 145-149.

[7] I. K. Lee, M. Jeun, H. J. Jang, W. J. Cho, K. H. Lee, A self-amplified transistor immunosensor under dual gate operation: highly sensitive detection of hepatitis B surface antigen, Nanoscale 7 (2015) 16789-16797.

[8] H. W. Jung, Y. W. Chang, G. Y. Lee, S. Cho, M. J. Kang, J. C. Pyun, A capacitive biosensor based on an interdigitated electrode with nanoislands, Anal. Chim. Acta 844 (2014) 27-34.

[9] Y. H. Choi, G. Y. Lee, H. Ko, Y. W. Chang, M. J. Kang, J. C. Pyun, Development of SPR biosensor for the detection of human hepatitis B virus using plasma-treated parylene-N film, Biosens. Bioelectron.56 (2014) 286-294.

[10] H. Imamura, Y. Matsuyama, E. Tanaka, T. Ohkubo, K. Hasegawa, S. Miyagawa, Y. Sugawara, M. Minagawa, T. Takayama, S. Kawasaki, M. Makuuchi, Risk factors contributing to early and late phase intrahepatic recurrence of hepatocellular carcinoma after hepatectomy, J. Hepatol. 38 (2003) 200-207.

[11] L. E. Ahangar, M. A. Mehrgardi, Amplified detection of hepatitis B virus using an electrochemical DNA biosensor on a nanoporous gold platform. Bioelectrochemistry 117 (2017) 83-88.

[12] J. W. Chung, S. D. Kim, R. Bernhardt, J. C. Pyun, Application of SPR biosensor for medical diagnostics of human hepatitis B virus (hHBV). Sensors and Actuators, B 111 (2005) 416-422.

[13] J. Wang, Z. Liu, C. Hu, S. Hu, Ultrasensitive photoelectrochemical biosensing of multiple biomarkers on a single electrode by a light addressing strategy. Anal. Chem. 87 (2015) 9368-9375.

[14] C. Altay, R. H. Senay, E. Eksin, G. Congur, A. Erdem, S. Akgol, Development of amino functionalized carbon coated magnetic nanoparticles and their application to electrochemical detection of hybridization of nucleic acids, Talanta 164 (2017) 175-182.

[15] Y. Xiao, Y. Sheng, J. Zhou, M. Chen, W. Wen, X. Zhang, S. Wang, A novel label-free strategy for pathogenic DNA detection based on metal ion binding-induced fluorescence quenching of graphitic carbon nitride nanosheets, Analyst 142 (2017) 2617-2623.

[16] J. Hu, C. Y. Wen, Z. L. Zhang, M. Xie, J. Hu, M. Wu, D. W. Pang, Optically encoded multifunctional nanospheres for one-pot separation and detection of multiplex DNA sequences, Anal. Chem. 85 (2013) 11929-11935.

[17] Y. Li, S. Liu, Q. Deng, L. Ling, A sensitive colorimetric DNA biosensor for specific detection of the HBV gene based on silver-coated glass slide and G-quadruplex-hemin DNAzyme. J. Med. Virol **2017**.

[18] L. Ding, J.You, R. Kong, F. Qu, Signal amplification strategy for sensitive immunoassay of Prostate Specific Antigen (PSA) based on ferrocene incorporated polystyrene spheres, Anal. Chim. Acta 793 (2013) 19-25.

[19] H. Pei, S. Zhu, M. Yang, R. Kong, Y. Zheng, F. Qu, Graphene oxide quantum dots@silver core-shell nanocrystals as turn-on fluorescent nanoprobe for ultrasensitive detection of Prostate Specific Antigen, Biosens. Bioelectron. 74 (2015) 909-914.

[20] Y. Jiang, X. Yang, C. Ma, C. Wang, Y. Chen, F. Dong, B. Yang, K. Yu, Q. Lin, Interfacing a tetraphenylethene derivative and a smart hydrogel for temperature-dependent photoluminescence with sensitive thermoresponse, ACS Appl. Mater. Interfaces 6 (2014) 4650-4657.

[21] H. Xie, F. Zeng, S. Wu, Ratiometric fluorescent biosensor for hyaluronidase with hyaluronan as both nanoparticle scaffold and substrate for enzymatic reaction, Biomacromolecules 15 (2014) 3383-3389.

[22] X. Huang, R. Chen, H. Xu, W. Lai, Y. Xiong, Nanospherical brush as catalase container for enhancing the detection sensitivity of competitive plasmonic ELISA. Anal. Chem. 88 (2016) 1951-1958.

[23] H. Han, L. Li, W. Wang, Y. Tian, Y. Wang, J. Wang, R. von Klitzing, X. Guo, Core-shell-corona silica hybrid nanoparticles templated by spherical polyelectrolyte brushes: a study by small angle X-ray scattering, Langmuir 33 (2017) 9857-9865.

[24] W. Jiang, Y. Lu, H. Wang, M. Wang, H. Yin, Amperometric biosensor for 5-hydroxymethylcytosine based on enzymatic catalysis and using spherical poly(acrylic acid) brushes, Microchim. Acta 184 (2017), 3789-3796.

[25] S. Cabana, C. Sofia Lecona-Vargas, H. Ivan Melendez-Ortiz, A. Contreras-Garcia, S. Barbosa, P. Taboada, B. Magarinos, E. Bucio, A. Concheiro, C. Alvarez-Lorenzo, Silicone rubber films functionalized with poly(acrylic acid) nanobrushes for immobilization of gold nanoparticles and photothermal therapy, J. Drug Deliv. Sci. Tec. 42 (2017) 245-254.

[26] Z. Li, M. Tang, W. Bai, R. Bai, Preparation of hydrophilic encapsulated carbon nanotubes with polymer brushes and its application in composite hydrogels, Langmuir

33 (2017), 6092-6101.

[27] J. Dai, Z. Bao, L. Sun, S. U. Hong, G. L. Baker, M. L. Bruening, High-capacity binding of proteins by poly(acrylic acid) brushes and their derivatives, Langmuir 22 (2006) 4274-4281.

[28] A. Dolatkhah, L. D. Wilson, Magnetite/polymer brush nanocomposites with switchable uptake behavior toward methylene blue, ACS Appl. Mater. Interfaces 8 (2016) 5595-5607.

[29] Z. Qu, F. Hu, K. Chen, Z. Duan, H. Gu, H. Xu, A facile route to the synthesis of spherical poly(acrylic acid) brushes via RAFT polymerization for high-capacity protein immobilization. J. Colloid Interface Sci. 398 (2013) 82-87.

[30] Y. Shao, L. Zhou, C. Bao, J. Ma, M. Liu, F. Wang, Magnetic responsive metal–organic frameworks nanosphere with core–shell structure for highly efficient removal of methylene blue, Chem. Eng. J. 283 (2016) 1127-1136.

[31] A. Grotzky, T. Nauser, H. Erdogan, A. D. Schlueter, P. Walde, A fluorescently labeled dendronized polymer-enzyme conjugate carrying multiple copies of two different types of active enzymes, J. Am. Chem. Soc. 134 (2012) 11392-11395.

[32] X. Pang, L. Zhao, M. Akinc, J. K. Kim, Z. Lin, Novel amphiphilic multi-arm, star-like block copolymers as unimolecular micelles, Macromolecules 44 (2011) 3746-3752.

[33] X. Pang, L. Zhao, W. Han, X. Xin, Z. Lin, A general and robust strategy for the synthesis of nearly monodisperse colloidal nanocrystals, Nature Nanotech. 8 (2013) 426-431.

[34] L. Gao, H. Zhang, H. Cui, A general strategy to prepare homogeneous and reagentless GO/lucigenin enzyme biosensors for detection of small biomolecules. Biosens. Bioelectron. 57 (2014) 65-70.

[35] W. Lai, D. Tang, J. Zhuang, G. Chen, H. Yang, Magnetic bead-based enzyme-chromogenic substrate system for ultrasensitive colorimetric immunoassay accompanying cascade reaction for enzymatic formation of squaric acid-iron(III) chelate, Anal. Chem. 86 (2014) 5061-5068.

[36] D. Liu, J. Yang, H. F. Wang, Z. Wang, X. Huang, Z. Wang, G. Niu, A. R. Hight

Walker, X. Chen, Glucose oxidase-catalyzed growth of gold nanoparticles enables quantitative detection of attomolar cancer biomarkers, Anal. Chem. 86 (2014) 5800-5806.

[37] Y. Xiong, Y. Zhang, P. Rong, J. Yang, W. Wang, D. Liu, A high-throughput colorimetric assay for glucose detection based on glucose oxidase-catalyzed enlargement of gold nanoparticles, Nanoscale 7 (2015) 15584-15588.

[38] W. Haiss, N. T. K. Thanh, J. Aveyard, D. G. Fernig, Determination of size and concentration of gold nanoparticles from UV-Vis spectra, Anal. Chem. 79 (2007) 4215-4221.

[39] H. Pei, Y. Zheng, R. Kong, L. Xia, F. Qu, Niche nanoparticle-based FRET assay for bleomycin detection via DNA scission, Biosens. Bioelectron. 85 (2016) 76-82.

[40] W. Wang, Y. Zhang, Q. Yang, M. Sun, X. Fei, Y. Song, Y. Zhang, Y. Li, Fluorescent and colorimetric magnetic microspheres as nanosensors for Hg^{2+} in aqueous solution prepared by a sol-gel grafting reaction and host-guest interaction, Nanoscale 5 (2013) 4958-4965.

[41] J. Li, H. Xiao, An efficient synthetic-route to prepare [2,3,6-tri-O-(2-bromo-2-methylpropionyl]-β-cyclodextrin), Tetrahedron Lett. 46 (2005), 2227-2229.

[42] F. A. Plamper, H. Becker, M. Lanzendorfer, M. Patel, A. Wittemann, M. Ballauff, A. H. E. Muller, Synthesis, characterization and behavior in aqueous solution of star-shaped poly(acrylic acid), Macromol. Chem. Phys. 206 (2005) 1813-1825.

[43] D. G. Duff, A. Baiker, P. P. Edwards, A new hydrosol of gold clusters 1 formation and particle-size variation, Langmuir 9 (1993), 2301-2309.

[44] Y. Zhao, Y. Q. Zheng, R. M. Kong, L. Xia, F. L. Qu, Ultrasensitive electrochemical immunosensor based on horseradish peroxidase (HRP)-loaded silica-poly(acrylic acid) brushes for protein biomarker detection, Biosens. Bioelectron. 75 (2016) 383-388.

[45] L. Huang, S. Dolai, K. Raja, M. Kruk, "Click" grafting of high loading of polymers and monosaccharides on surface of ordered mesoporous silica, Langmuir 26 (2010) 2688-2693.

[46] L. Wang, H. Zou, Z. Dong, L. Zhou, J. Li, Q. Luo, J. Zhu, J. Xu, J. Liu, Temperature-driven switching of the catalytic activity of artificial glutathione peroxidase by the shape transition between the nanotubes and vesicle-like structures, Langmuir 30 (2014) 4013-4018.

[47] X. Fan, L. Wang, Q. Luo, L. Zhao, J. Xu, J. Liu, Q. Zheng, Construction of giant branched nanotubes from cyclodextrin-based supramolecular amphiphiles, Chem. Commun. 51 (2015) 6512-6514.

[48] Y. X. Wang, Y. M. Zhang, Y. Liu, Photolysis of an amphiphilic assembly by calixarene-induced aggregation, J. Am. Chem. Soc. 137 (2015) 4543-4549.

[49] Y. Zhao, Y. Wang, X. B. Zhang, R. M. Kong, L. Xia, F. L. Qu, Cascade enzymatic catalysis in poly(acrylic acid) brushes-nanospherical silica for glucose detection, Talanta 155 (2016) 265-271.

[50] B. Smitha, S. Sridhar, A. A. Khan, Polyelectrolyte complexes of chitosan and poly(acrylic acid) as proton exchange membranes for fuel cells, Macromolecules 37 (2004) 2233-2239.

[51] L. Ding, Z. Qin, C. Xiang, G. Zhou, Novel fluorescent organic nanoparticles as a label-Free biosensor for dopamine in serum, J. Mater. Chem. B 5 (2017) 2750-2756.

[52] F. Thielbeer, K. Donaldson, M. Bradley, Zeta potential mediated reaction monitoring on nano and microparticles, Bioconjugate Chem. 22 (2011) 144-150.

Research Highlights

Controllable molecular weight poly(acrylic acid) brushes.

Host-Guest Interactions of *β*-CD-PAA and Ad-SiO_2.

Signal amplification was achieved using SiO_2@PAA/GOx.

Colorimetric bioassay was designed for the ultrasensitive detection of Hepatitis B Virus DNA sequence